

Heterocyclic Radicals in the Gas Phase. An Experimental and Computational Study of 3-Hydroxypyridinium Radicals and Cations

Jill K. Wolken and František Tureček*

Contribution from the Department of Chemistry, Bagley Hall, Box 351700, University of Washington, Seattle, Washington 98195-1700

Received October 30, 1998

Abstract: Radicals 3-hydroxy-(1*H*)-pyridinium (**1H**) through 3-hydroxy-(6*H*)-pyridinium (**6H**) and 3-pyridylhydroxonium (**7H**) were studied as models of hydrogen atom adducts to nitrogen heterocycles. Radical **1H** was generated in the gas phase by femtosecond collisional electron transfer to stable 3-hydroxy-(1*H*)-pyridinium cations (**1H**⁺). The fractions of nondissociating **1H** decreased with increasing internal energies of the precursor cations as determined by the gas-phase protonation energetics. Radical **1H** dissociated unimolecularly by loss of the N-bound hydrogen atom to produce 3-hydroxypyridine (**1**). The dissociation showed large isotope effects that depended on the radical's internal energy. Other dissociations of **1H** were loss of OH•, ring contraction forming C–OH and pyrrole, and ring cleavages leading to C₃H_x and C₂H_xN fragments. Combined MP2 and B3LYP/6-311G(2d,p) calculations yielded topical proton affinities in **1** as 938 (N-1), 757 (C-2), 649 (C-3), 721 (OH), 727 (C-4), 714 (C-5), and 763 (C-6) kJ mol⁻¹. **1H**⁺ was the most stable ion isomer formed by protonation of **1**. Radical **1H** was the most stable isomer whereas **2H**, **3H**, **4H**, **5H**, and **6H** were calculated to be 9, 48, 16, 18, and 22 kJ mol⁻¹ less stable than **1H**, respectively. The 3-pyridylhydroxonium radical **7H** dissociated without barrier by cleavage of the O–H bond. N–H bond dissociation in **1H** was 102 kJ mol⁻¹ endothermic at 298 K and required an activation energy of 126 kJ mol⁻¹. Deuterium isotope effects on the N–(H,D) bond dissociations were modeled by RRKM calculations and used to estimate the internal energy distribution in **1H**. Isomerizations of **1H** to **2H** and **2H** to **3H** required activation energies of 174 and 130 kJ mol⁻¹, respectively. Ring-cleavage dissociations of **1H** were >220 kJ mol⁻¹ endothermic. The occurrence of competitive ring cleavage dissociations pointed to a bimodal internal energy distribution in **1H** due to the formation of excited electronic states upon electron transfer. The electronic properties and excited states of heterocyclic radicals are discussed.

Introduction

Additions of small radicals to aromatic and heterocyclic molecules are fundamental to processes as diverse as tropospheric oxidation¹ and radiation damage.² Whereas the reactions of heteroaromatics (**M**) with radiatively, chemically, or photochemically generated OH• and H• radicals have been studied in much detail,² little is known about the structure and energetics of radical intermediates of the general formulas (**M** + OH)• and (**M** + H)•. Radical additions has been studied in the gas phase,¹ solution,² or frozen matrix;³ of these the gas phase appears to be an ideal environment for studying the *intrinsic properties* of heterocyclic radicals. We have reported recently on the preparation of several heterocyclic radicals in the gas phase,^{4–9} as reviewed.⁷ The general strategy to generate

(1) See for example: Atkinson, R. *J. Phys. Chem. Ref. Data, Monogr.* **1994**, 2, 47–58.

(2) For reviews see: (a) von Sonntag, C. In *Physical and Chemical Mechanisms in Molecular Radiation Biology*; Glass, W. A., Varma, M. N., Eds.; Plenum Press: New York, 1991; pp 287–321. (b) Steenken, S. *Chem. Rev.* **1989**, 89, 503.

(3) (a) Cullis, P. M.; Malone, M. E.; Podmore, I. D.; Symons, M. C. R. *J. Phys. Chem.* **1995**, 99, 9293. (b) Symons, M. C. R. *J. Chem. Soc., Faraday Trans. 1* **1987**, 83, 1.

(4) Nguyen, V. Q.; Turecek, F. *J. Mass Spectrom.* **1996**, 31, 1173.

(5) Nguyen, V. Q.; Turecek, F. *J. Mass Spectrom.* **1997**, 32, 55.

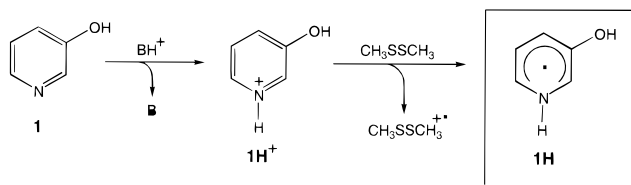
(6) Nguyen, V. Q.; Turecek, F. *J. Am. Chem. Soc.* **1997**, 119, 2280.

(7) Turecek, F. *J. Mass Spectrom.* **1998**, 33, 779.

(8) Turecek, F.; Wolken, J. K.; Sadilek, M. *Eur. Mass Spectrom.* **1998**, 4, 321.

(9) Turecek, F.; Wolken, J. K. *J. Phys. Chem. A* **1999**, 103, 1905.

Scheme 1



heterocyclic radicals of the (**M** + H)• type relies on the methods of neutralization–reionization mass spectrometry (NRMS)¹⁰ as shown for 3-hydroxypyridine (**1**) in Scheme 1.

A corresponding stable cation is prepared first by gas-phase protonation of the heterocycle. The gas-phase acid is chosen such as to provide some degree of protonation selectivity. For example, a weak acid is chosen such as to attack exclusively the most basic site in the heterocycle molecule, or a series of stronger acids can be used to attack sites of gradually decreasing basicities.^{4–6} The stable ions are accelerated to kiloelectronvolt kinetic energies and discharged by collisions with an electron

(10) For reviews see: (a) Wesdemiotis, C.; McLafferty, F. W. *Chem. Rev.* **1987**, 87, 485. (b) Terlouw, J. K.; Schwarz, H. *Angew. Chem., Int. Ed. Engl.* **1987**, 26, 805. (c) Holmes, J. L. *Mass Spectrom. Rev.* **1989**, 8, 513. (d) Terlouw, J. K. *Adv. Mass Spectrom.* **1989**, 11, 984. (e) McLafferty, F. W. *Science* **1990**, 247, 925. (f) Turecek, F. *Org. Mass Spectrom.* **1992**, 27, 1087. (g) Goldberg, N.; Schwarz, H. *Acc. Chem. Res.* **1994**, 27, 347. (h) Schalley, C. A.; Hornung, G.; Schroder, D.; Schwarz, H. *Chem. Soc. Rev.* **1998**, 27, 91.

donor under conditions that favor each ion undergoing a single collision. Polarizable molecules such as dimethyl disulfide¹¹ are used as electron donors. Since the ion–molecule interaction during collisional electron transfer at kiloelectronvolt collision energies lasts only a few femtoseconds,^{10c} the structure of the cation is almost exactly copied on to the nascent radical. Unimolecular radical reactions, such as dissociations and rearrangements, are observed over the time scale of several microseconds, and the products are analyzed after collisional reionization to cations. Radical reactions can be further promoted by collisional activation of the neutral intermediates following their formation by electron transfer.¹² Varying the time scales for radical and ion dissociations (variable-time NRMS)¹³ allows one to distinguish these two types of reactions even if they produce chemically identical species.¹¹

In this paper we address by experiment the intrinsic properties of radical **1H** and use ab initio and density functional theory calculations to investigate a complete set of isomeric radicals **1H–7H** which correspond to hydrogen atom adducts to 3-hydroxypyridine (**1**). Previous studies established unambiguously that **1** exists as a single tautomer in the gas phase as studied by ab initio¹⁴ and semiempirical calculations¹⁵ and UV,¹⁶ IR,¹⁷ Raman,^{17c} photoelectron,¹⁸ and mass spectra.¹⁹ Preparation of transient radicals derived from **1** is therefore free of complications caused by the existence of two or more tautomers of the parent heterocycle. In a related paper²⁰ we addressed radicals derived from the more complicated 2-hydroxypyridine/2-pyridone tautomeric system.²¹

The properties of **1** in radical reactions in solution have been studied extensively.²² **1** is produced on radiolysis of pyridine, nicotinic acid, and pyridoxine derivatives. However, besides radiolytic studies in solution,²² there have been virtually no data pertinent to the structure, stabilities, and reactivity of transient radicals derived from **1**. In an early computational study, Mezey et al.²³ addressed the reaction pathway for addition of OH• to pyridine, which included a radical of the (**1** + H)• type.

(11) Sadilek, M.; Turecek, F. *J. Phys. Chem.* **1996**, *100*, 224.

(12) (a) Danis, P.; Feng, R.; McLafferty, F. W. *Anal. Chem.* **1986**, *58*, 348. (b) Turecek, F.; Drinkwater, D. E.; Maquestiau, A.; McLafferty, F. W. *Org. Mass Spectrom.* **1989**, *24*, 669. (c) Shaffer, S. A.; Turecek, F.; Cerny, R. L. *J. Am. Chem. Soc.* **1994**, *115*, 12117.

(13) (a) Kuhns, D. W.; Shaffer, S. A.; Tran, T. B.; Turecek, F. *J. Phys. Chem.* **1994**, *98*, 4845. (b) Kuhns, D. W.; Turecek, F. *Org. Mass Spectrom.* **1994**, *29*, 463.

(14) (a) Wang, J.; Boyd, R. J. *J. Phys. Chem.* **1996**, *100*, 16141. (b) Person, W. B.; Del Bene, J. E.; Szajda, W.; Szczepaniak, K.; Szczesniak, M. *J. Phys. Chem.* **1991**, *95*, 2770. (c) Scanlan, M. J.; Hillier, I. A.; MacDowell, A. A. *J. Am. Chem. Soc.* **1983**, *105*, 3568. (d) Scanlan, M. J.; Hillier, I. H.; Davies, R. H. *J. Chem. Soc., Chem. Commun.* **1982**, 685. (e) La Manna, G.; Venuti, E. *J. Comput. Chem.* **1982**, *3*, 593. (f) La Manna, G. *THEOCHEM* **1981**, *2*, 389. (g) Bodor, N.; Dewar, M. J. S.; Harget, A. *J. Am. Chem. Soc.* **1970**, *92*, 2929.

(15) Fabian, W. M. F. *J. Comput. Chem.* **1991**, *12*, 17.

(16) Metzler, D. E.; Harris, C. M.; Johnson, R. J.; Siano, D. B.; Thomson, J. A. *Biochemistry* **1973**, *12*, 5377. (b) Kwiatkowski, J. S. *J. Mol. Struct.* **1971**, *10*, 245. (c) Kwiatkowski, J. S. *Theor. Chim. Acta* **1970**, *16*, 243. (d) Gordon, A.; Katritzky, A. R. *Tetrahedron Lett.* **1968**, 2767.

(17) (a) Buyl, F.; Smets, J.; Maes, G.; Adamowicz, L. *J. Phys. Chem.* **1995**, *99*, 14967. (b) Rodionova, G. N.; Tuchin, Yu. G.; Partalla, N. A. *Khim. Geterotsikl. Soedin.* **1987**, 660. (c) Mehdi, K. C. *Indian J. Phys. B* **1984**, *58B*, 328.

(18) Cook, M. J.; El-Abbadly, S.; Katritzky, A. R.; Guimon, C.; Pfister-Guillouzo, G. *J. Chem. Soc., Perkin Trans. 2* **1977**, 1652.

(19) (a) Baldwin, M. A.; Langley, G. J. *J. Chem. Soc., Perkin Trans. 2* **1988**, 347. (b) Maquestiau, A.; van Haverbeke, Y.; Flammang, R.; Mispreuve, H.; Katritzky, A. R.; Ellison, J.; Frank, J.; Meszaros, Z. *J. Chem. Soc., Chem. Commun.* **1979**, 888. (c) Maquestiau, A.; VanHaverbeke, Y.; De Meyer, C.; Katritzky, A. R.; Cook, M. J.; Page, A. D. *Can. J. Chem.* **1975**, *53*, 490.

(20) Wolken, J. K.; Turecek, F. *J. Phys. Chem. A*. Accepted for publication.

(21) Katritzky, A. R.; Karelson, M.; Harris, P. A. *Heterocycles* **1991**, *32*, 329.

Experimental Section

Methods. Measurements were made on a tandem quadrupole acceleration–deceleration mass spectrometer as described previously.²⁴ Precursor cation radicals were generated by electron impact ionization (70 eV, 200–250 °C). Gas-phase protonation was achieved by ion–molecule reactions in a tight chemical-ionization ion source of our design.²⁴ CH₅⁺/CH₄, H₃O⁺/H₂O, (CH₃)₂C–OH⁺/acetone, and NH₄⁺/NH₃ were used as gas-phase acids for protonation. D₃O⁺/D₂O and ND₄⁺/ND₃ were used for deuteration combined with H/D exchange of the acidic hydroxyl proton in the substrate molecule. CD₅⁺/CD₄ and (CD₃)₂C–OD⁺/acetone-*d*₆ were used for gas-phase deuteration without OH/OD exchange. Stable ions of 8200 eV kinetic energy were neutralized by collisions with dimethyl disulfide at pressures allowing 70% transmittance of the precursor ion beam. The radical lifetimes were 4.67, 4.70, and 4.72 μs for (M + H)[•], (M + D)[•], and (MD + D)[•], respectively. The neutral products were reionized by collisions with oxygen (70% ion transmittance). Collisional activation of the radical intermediates (NCR)¹² was performed with helium at 70 or 50% transmittance of the precursor ion beam. The reported spectra are averages of 30–40 consecutive scans taken at a scan rate of 1 mass unit/s. The spectra were reproduced over the period of several weeks. Variable-time measurements were performed by varying the potentials on the drift region lens elements as described previously.¹³ The neutral lifetimes were 0.45, 1.32, 2.20, and 3.07 μs.

Collision-induced dissociations (CID) were measured on a JEOL HX-110 doubly focusing mass spectrometer of an EB geometry (electrostatic sector E precedes magnet B). Air was used as a collision gas at pressures allowing 50% transmittance of the ion beam at 10 keV. CAD spectra were measured in the first field-free region and the spectra were recorded with use of a linked B/E scan. The spectra were averaged over 10–12 consecutive scans. CAD spectra with mass-analyzed kinetic energy scans (MIKES) were also measured on the Copenhagen four-sector JEOL HX-110/HX-110 mass spectrometer using oxygen as collision gas at 70% precursor ion beam transmittance. The precursor ion was selected by the first two sectors (EB) at mass resolution ~3000.

Materials. 3-Hydroxypyridine (**1**, Aldrich) was used as received and sampled into the ion source from a heated glass direct probe. Dimethyl disulfide (Aldrich) was purified by several freeze–pump–thaw cycles before use. 3-Hydroxypyridine-OD (**1OD**) was prepared by repeated H/D exchange in D₂O, the solvent was evaporated with a stream of nitrogen, and the product was stored in a desiccator under nitrogen.

Calculations. Standard ab initio calculations were performed by using the Gaussian 94 suite of programs.²⁵ Geometries were optimized with Hartree–Fock calculations using the 6-31G(d,p) basis set unless stated otherwise. A spin-unrestricted formalism (UHF) was used for the radicals. The optimized structures were characterized by harmonic frequency analysis as minima (all frequencies real) or transition states (one imaginary frequency). The frequencies were corrected by 0.893²⁶ and used to calculate zero-point vibrational corrections and 298 K

(22) (a) Naik, D. B.; Moorthy, P. N. *J. Chem. Soc., Perkin Trans. 2* **1990**, 705. (b) Naik, D. B.; Moorthy, P. N. *J. Radioanal. Nucl. Chem.* **1991**, *148*, 403. (c) Anbar, M.; Meyerstein, D.; Neta, P. *J. Phys. Chem.* **1966**, *70*, 2660. (d) Neta, P.; Dorfman, L. M. *Adv. Chem. Ser.* **1968**, *81*, 222. (e) Cercek, P.; Ebert, M. *Trans. Faraday Soc.* **1967**, *67*, 1687. (f) Simic, M.; Ebert, M. *Int. J. Radiat. Phys. Chem.* **1971**, *3*, 259. (g) Steenken, S.; O'Neill, P. *J. Phys. Chem.* **1978**, *82*, 372. (h) Selvarajan, N.; Raghavan, N. V. *J. Phys. Chem.* **1980**, *84*, 2548.

(23) Anthony, M. C.; Waltz, W. L.; Mezey, P. G. *Can. J. Chem.* **1982**, *60*, 813.

(24) Turecek, F.; Gu, M.; Shaffer, S. A. *J. Am. Soc. Mass Spectrom.* **1992**, *3*, 493.

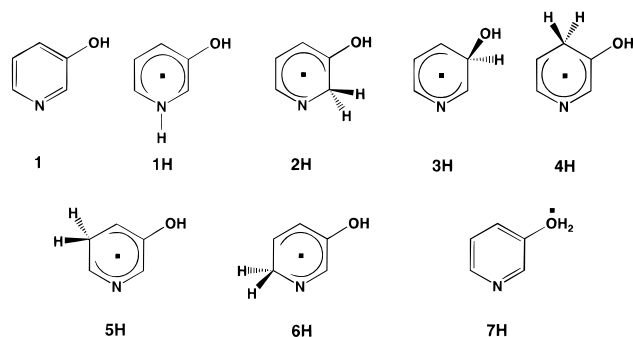
(25) *Gaussian 94* (Revisions B.2 and E.1); Frisch, M. J.; Trucks, G. W.; Schlegel, H. B.; Gill, P. M. W.; Johnson, B. G.; Robb, M. A.; Cheeseman, J. R.; Keith, T. A.; Petersson, G. A.; Montgomery, J. A.; Raghavachari, K.; Al-Laham, M. A.; Zakrzewski, V. G.; Ortiz, J. V.; Foresman, J. B.; Cioslowski, J.; Stefanov, B. B.; Nanayakkara, A.; Challacombe, M.; Peng, C. Y.; Ayala, P. Y.; Chen, W.; Wong, M. W.; Andres, J. L.; Replogle, E. S.; Gomperts, R.; Martin, R. L.; Fox, D. J.; Binkley, J. S.; Defrees, D. J.; Baker, J.; Stewart, J. P.; Head-Gordon, M.; Gonzalez, C.; Pople, J. A. Gaussian, Inc.: Pittsburgh, PA, 1995.

(26) Hehre, W. J.; Radom, L.; Schleyer, P. v. R.; Pople, J. A. *Ab Initio Molecular Orbital Theory*, Wiley: New York, 1986; pp 228–236.

enthalpies. Complete optimized geometries (Cartesian coordinates) and uncorrected harmonic frequencies for all species are given as Supporting Information. Single-point energies were calculated with the Moller–Plesset perturbational theory²⁷ truncated at second order (MP2) with use of frozen core excitations. Contamination by higher spin states in UHF and UMP2 calculations was corrected in part by Schlegel's spin annihilation procedure.²⁸ Another set of single-point energies was calculated with density functional theory by using Becke's three-parameter hybrid functional (B3LYP).²⁹ Both sets of single-point calculations used the larger 6-311G(2d,p) basis set, which had been shown previously to provide reasonably accurate relative energies and proton affinities for several ionic and radical heterocyclic systems.^{4–7,9} Relative energies for radicals, transition states, and dissociation energies were obtained by averaging the spin-projected MP2 (PMP2) and B3LYP energies. This empirical procedure corrects for radical overstabilization by DFT methods³⁰ and destabilization by ab initio methods due to residual spin-contamination in PMP2 energies. RRKM calculations were performed by using Hase's program³¹ as described in detail previously.⁹

Results and Discussion

Ion Formation and Dissociations. Precursor ions for the formation of radicals **1H** were prepared by gas-phase protonation of **1**. According to the proton affinities of the reagent gases³² and **1**, PA(**1**) = 922 kJ mol⁻¹,³³ protonations with CH₅⁺, H₃O⁺, (CH₃)₂C–OH⁺, and NH₄⁺ were 378, 232, 110, and 69 kJ mol⁻¹ exothermic, provided they occurred at the most basic site in **1**. Stable (**1** + H)⁺ ions were obtained in each case, which were used for radical generation by collisional electron transfer.



To characterize the precursor ions, ab initio and DFT calculations were performed to obtain topical proton affinities in **1**.³⁴ Table 1 shows the calculated topical PA values,⁷ which confirmed that the nitrogen atom was the most basic site in **1**. The calculated thermodynamic proton affinity of **1** to form the

(27) Moller, C.; Plesset, M. S. *Phys. Rev.* **1934**, *46*, 618.

(28) (a) Mayer, I. *Adv. Quantum Chem.* **1980**, *12*, 189. (b) Schlegel, H. B. *J. Chem. Phys.* **1986**, *84*, 4530.

(29) (a) Becke, A. D. *J. Chem. Phys.* **1993**, *98*, 1373 and 5648. (b) Stephens, P. J.; Devlin, F. J.; Chablowski, C. F.; Frisch, M. J. *J. Phys. Chem.* **1994**, *98*, 11623.

(30) Nguyen, M. T.; Creve, S.; Vanquickenborne, L. G. *J. Phys. Chem.* **1996**, *100*, 18422.

(31) (a) Zhu, L.; Hase, W. L. *Quantum Chemistry Program Exchange*; Indiana University: Bloomington, IN, 1994; Program No. QCPE 644. (b) Zhu, L.; Hase, W. L. *Chem. Phys. Lett.* **1990**, *175*, 117.

(32) The proton affinities for the reagent gases (kJ mol⁻¹) were taken from the following: Mallard, W. G.; Lindstrom, P. J., Eds. *NIST Chemistry Webbook, NIST Standard Reference Database*; NIST: Gaithersburg, MD, 1998; No. 69. <http://webbook.nist.gov/chemistry>: CH₄ (544), H₂O (690), acetone (812), and ammonia (854).

(33) Aue, D. H.; Webb, H. M.; Davidson, W. R.; Toure, P.; Hopkins, H. P., Jr.; Moulik, S. P.; Jahagirdar, D. V. *J. Am. Chem. Soc.* **1991**, *113*, 1770.

(34) For earlier proton affinity calculations that included **1** see: (a) Catalan, J.; Mo, O.; Perez, P.; Yanez, M. *J. Am. Chem. Soc.* **1979**, *101*, 6520. (b) Brown, R. S.; Tse, A. *Can. J. Chem.* **1980**, *58*, 694. (c) Butt, G.; Topsom, R. D.; Taft, R. W. *THEOCHEM* **1987**, *38*, 141. (d) Reynolds, W. F.; Mezey, P. G.; Hehre, W. J.; Topsom, R. D.; Taft, R. W. *J. Am. Chem. Soc.* **1977**, *99*, 5821.

Table 1. Topical Proton Affinities in 3-Hydroxypyridine

position	PA ^a		-ΔH _{r,298} ^b			
	MP2	B3LYP	NH ₄ ⁺	(CH ₃) ₂ C–OH ⁺	H ₃ O ⁺	CH ₅ ⁺
N-1	931	946	85	126	249	395
C-2	738	776	– ^c	–	67	213
C-3	628	670	–	–	–	105
C-4	706	748	–	–	37	183
C-5	691	737	–	–	24	170
C-6	743	782	–	–	72	219
O	715	726	–	–	31	177

^a In units of kJ mol⁻¹. ^b Reaction enthalpies for exothermic protonations based on the averaged MP2 and B3LYP topical proton affinities in **1** and experimental proton affinities of NH₃ (854 kJ mol⁻¹), acetone (812 kJ mol⁻¹), H₂O (690 kJ mol⁻¹), and methane (544 kJ mol⁻¹). ^c Endothermic protonations.

most stable ion **1H**⁺, 931 and 946 kJ mol⁻¹ by MP2 and B3LYP, respectively, was in reasonably good agreement with the experimental value (vide supra).³³ Since only exothermic protonations are efficient under chemical ionization conditions,³⁵ the topical PA values determine which of the positions in **1** can be attacked by the gas-phase acid used. Table 1 shows that protonations with NH₄⁺ and (CH₃)₂C–OH⁺ can occur exothermically at the nitrogen atom only and should thus produce ions **1H**⁺ exclusively. Protonation with H₃O⁺ was predicted to be less selective in that it could occur at all positions in **1** except C-3. Protonation of C-5 by H₃O⁺ was energetically borderline (exothermic by B3LYP but endothermic by MP2, Table 1) and may not be competitive with protonations at the other more basic positions in **1**. Protonation by CH₅⁺ was exothermic for all positions in **1** and was expected to show the lowest selectivity.

To elucidate ion dissociations, collisionally activated spectra were investigated for **1H**⁺ by protonation with (CH₃)₂C–OH⁺, **1D**⁺ by deuteration with (CD₃)₂C–OD⁺, **1ODH**⁺ by protonation of **1OD** with (CH₃)₂C–OH⁺, and **1ODD**⁺ by deuteration of **1OD** with (CD₃)₂C–OD⁺. The major dissociation channels of **1H**⁺ were loss of H, H₂, OH, H₂O, and COH and formation of C₂H₄N⁺, C₃H₃⁺, and HC=NH⁺ (Figure 1). The loss of H from **1H**⁺ was nonspecific and involved hydrogen atoms from all positions. For example, **1D**⁺ showed loss of H and D in a 80/20 ratio (Figure 1), which indicated involvement of the ring hydrogen atoms. The MIKES–CAD spectra of **1ODH**⁺ and **1ODD**⁺ (not shown) showed essentially random losses of H and D. The elimination of COH from **1H**⁺ involved the hydroxyl hydrogen, as deduced from deuterium labeling in **1ODH**⁺. The structure of the resulting C₄H₅N⁺ ion from **1H**⁺ was probed by NRMS, which gave a spectrum identical with that of pyrrole⁺.^{4,36} The loss of hydroxyl from **1H**⁺ involved partial exchange of the OH hydrogen with those of the ring C–H bonds.

In summary, the CAD spectra provided signatures for ion dissociations to be distinguished in the NR mass spectra. In particular, the ion dissociations were characterized by nonspecific loss of hydrogen atoms from **1H**⁺. In addition, small neutral fragments originating from CAD of the precursor ion were identified.

Formation and Dissociations of Radicals 1H•. Collisional neutralization was studied for ions prepared by protonation of **1** with NH₄⁺, (CH₃)₂C–OH⁺, H₃O⁺, and CH₅⁺ of increasing exothermicity. The NR mass spectra (Figure 2) showed non-

(35) (a) Bohme, D. K.; Mackay, G. I.; Schiff, H. I. *J. Chem. Phys.* **1980**, *73*, 4976. For a review see: (b) Harrison, A. G. *Chemical Ionization Mass Spectrometry*, 2nd ed.; CRC Press: Boca Raton, 1992; pp 17–18.

(36) For structure elucidation of C₄H₅N⁺ ions formed from **1** see: (a) Sakurai, H.; Jennings, K. R. *Org. Mass Spectrom.* **1981**, *16*, 393. (b) Van Tilborg, M. W. E. M.; Van Thuijl, J. *Org. Mass Spectrom.* **1983**, *18*, 331.

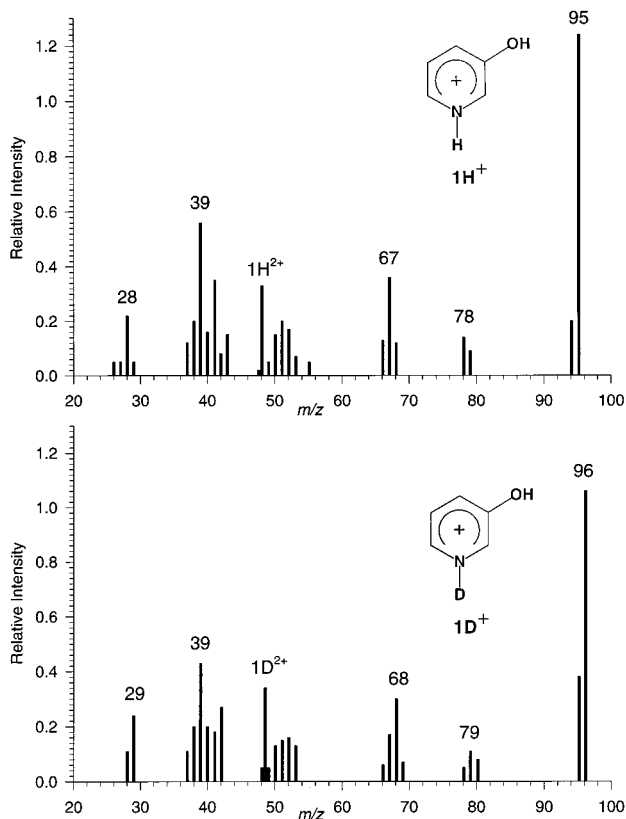


Figure 1. Collision-induced dissociation mass spectra of 1H^+ and 1D^+ at 10 keV ion kinetic energy. Air at 50% ion beam transmittance was used as a collision gas.

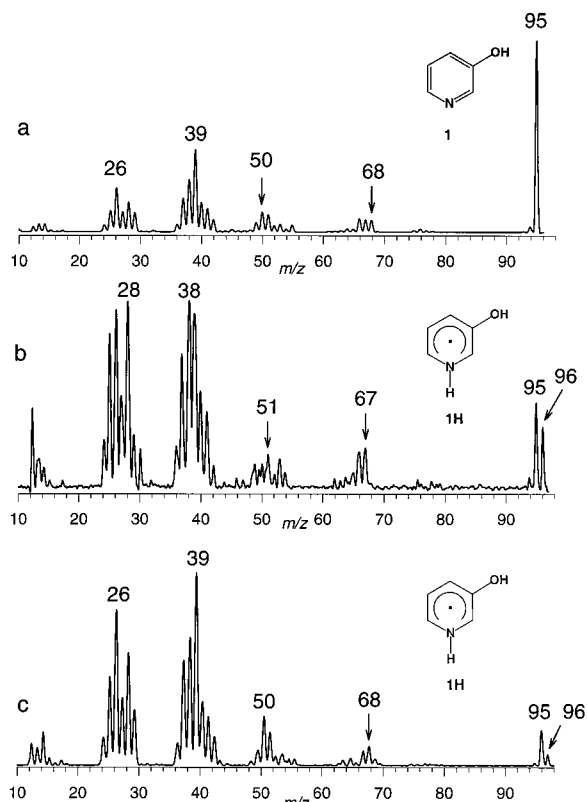


Figure 2. Neutralization (CH_3SSCH_3 , 70% transmittance)—reionization (O_2 , 70% transmittance) spectra of (a, top) **1**, (b, middle) 1H^+ by protonation with NH_4^+ , and (c, bottom) 1H^+ by protonation with CH_5^+ .

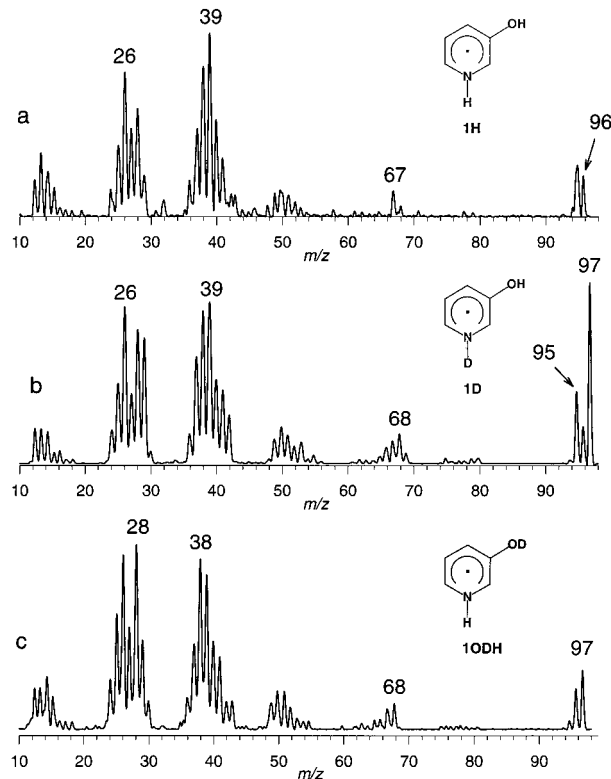


Figure 3. Neutralization (CH_3SSCH_3 , 70% transmittance)—reionization (O_2 , 70% transmittance) spectra of (a, top) 1H^+ by protonation of **1** with $(\text{CH}_3)_2\text{C}-\text{OH}^+$, (b, middle) 1D^+ by deuteration of **1** with $(\text{CD}_3)_2\text{C}-\text{OD}^+$, and (c, bottom) 1ODH^+ by protonation of **1OD** with $(\text{CH}_3)_2\text{C}-\text{OH}^+$.

lifetimes greater than the flight time between the neutralizing and reionizing collisions ($4.67 \mu\text{s}$). The relative abundances of the survivor ions, expressed as $[1\text{H}] = I(1\text{H}^+)/\sum I_{\text{NR}}$,³⁷ correlated with the precursor ion internal energies. The latter are limited from above by the difference between the proton affinity of **1** and that of the conjugated base of the gas-phase acid (Table 1). The NR spectra showed $[1\text{H}] = 2.0, 1.8, 1.1,$ and 0.6% for precursor ions prepared by protonations with NH_4^+ , $(\text{CH}_3)_2\text{C}-\text{OH}^+$, H_3O^+ , and CH_5^+ , respectively. The dissociations induced by NR were loss of H (m/z 95), CO (m/z 68), and COH (m/z 67) and formation of small fragments, $\text{C}_2\text{H}_2/\text{CN}$ (m/z 26), CO, COH, $\text{C}_3\text{H}_3/\text{C}_2\text{HN}$ (m/z 39), and $\text{C}_4\text{H}_x/\text{C}_3\text{NH}_y$ (m/z 49–55). Some of these fragments coincided by mass with those from collisionally activated ion dissociations and could occur after collisional reionization. However, some dissociations of intermediate radicals showed distinct mechanisms and could be distinguished by deuterium labeling.

Deuterium labeling at N (1D^+) had a major effect on the stability of the survivor ion in the NR mass spectrum (Figure 3) and resulted in a substantially increased $[1\text{D}] = 7.1\%$ compared with 1.8% for 1H^+ (vide supra). By contrast, deuterium labeling in the hydroxy group had a smaller stabilizing effect, $[1\text{ODH}] = 2.4\%$. The isotope effects observed for 1ODD^+ prepared by deuteration with ND_4^+ and D_3O^+ (spectra not shown) were similar to that for 1D^+ .

Deuterium labeling at N and in the hydroxyl group revealed the mechanism of hydrogen atom loss from 3-hydroxypyridinium radicals. Table 2 shows the fractions of H and D from deuterated ions upon NR. In contrast to ion dissociations, the NR dissociations showed substantial specificity

(37) $I(1\text{H}^+)$ is the intensity of the survivor ion, $\sum I_{\text{NR}}$ is the sum of all ion intensities in the NR mass spectrum.

Table 2. Fractions of H and D Loss from **1H**, **1D**, **1ODH**, and **1ODD**

reagent	ion	loss of H/D (%)	
		-H	-D
ND ₄ ⁺	1ODD ⁺	15	85
(CD ₃) ₂ C-OD ⁺	1D ⁺	35	65
		24 ^a	76 ^a
(CH ₃) ₂ C-OH ⁺	1ODH ⁺	86	14
D ₃ O ⁺	1ODD ⁺	16	84
CD ₅ ⁺	1D ⁺	31	69
CH ₅ ⁺	1ODH ⁺	91	9

^a From collisional activation of intermediate radicals **1D**.

Table 3. Relative Energies of Ions **1H**⁺–**7H**⁺ and Radicals **1H**–**6H**

species	relative energy ^a	
	PMP2	B3LYP
ions		
1H ⁺	0	0
2H ⁺	192	170
3H ⁺	303	276
4H ⁺	224	197
5H ⁺	239	209
6H ⁺	188	164
7H ⁺	215	219
radicals		
1H	0	0
2H	9	8
3H	43	53
4H	16	16
5H	14	21
6H	21	22

^a In kJ mol⁻¹ from single-point calculations with the 6-311G(2d,p) basis set and HF/6-31G(d,p) zero point and 298 K thermal corrections.

in the loss of the nitrogen-bound hydrogen atom. Loss of H or D from the hydroxyl group was less effective (Table 3). About 15% of H loss was due to hydrogens from ring positions other than nitrogen as evidenced by the data for **1ODD**.

For the selectively labeled ion **1D**⁺ the specific loss of the nitrogen-bound deuterium atom was further increased to 76% upon collisional activation of intermediate radicals **1D** (Figure 4a,b). A similar effect was observed for variable-time experiments in which the observation time for neutral dissociations was increased from 0.45 to 1.32 μs (Figure 4c,d). Both the extent of (H,D) loss and the [**1D** - D]/[**1D** - H] abundance ratios increased upon allowing a longer time for neutral dissociations while shortening the time for ion dissociations. The effects of neutral collisional activation and lifetime clearly pointed out that *the specific loss of H was due to dissociations of neutral 1H* or its isotopomers.

The NR spectra for **1ODD**⁺ and **1D**⁺ formed by exothermic deuteronations with D₃O⁺ and CD₅⁺ also showed predominant losses of D (Table 2). Deuteronations with CD₅⁺ were sufficiently exothermic to occur nonselectively at the C-2 through C-6 positions in **1** to give ions **2D**⁺ through **6D**⁺, or at the hydroxy group to give ion **7D**⁺. Likewise, deuteronation with D₃O⁺, when accompanied by OH → OD exchange, should produce ions **2ODD**⁺, **4ODD**⁺, **5ODD**⁺, **6ODD**⁺, and **7ODD**⁺ nonselectively. Collisional neutralization of these ions, followed by dissociation of the radical intermediates, would be expected to yield >50/50 ratios for the H/D loss from **2D** through **7D**, and **2ODD** through **6ODD**, because the geminal H and D atoms in these radicals would be chemically equivalent and the loss of H would be preferred by a primary isotope effect. The fact that this was not observed presented evidence that isomers other

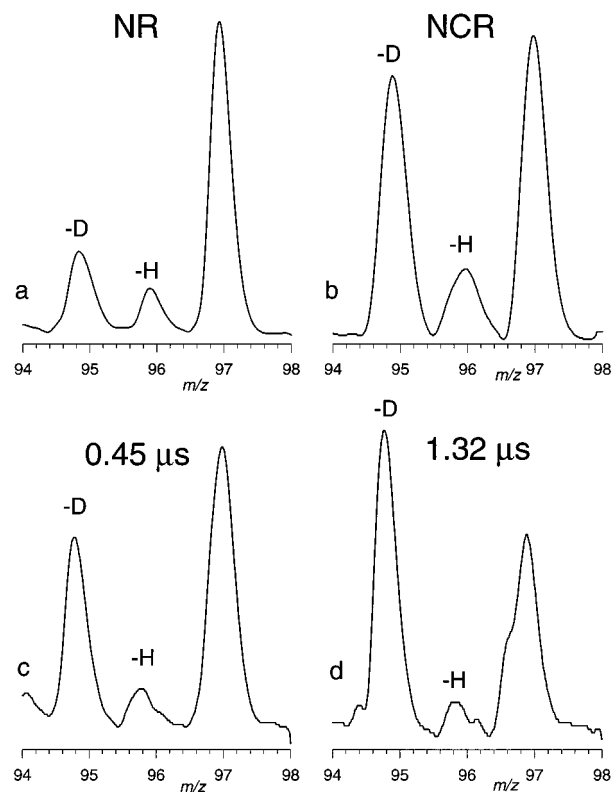


Figure 4. Molecular ion regions in the NR mass spectra of **1D**⁺: (a) neutralization (CH₃SSCH₃, 70% transmittance)-reionization (O₂, 70% transmittance); (b) neutralization-collisional activation (He, 50% transmittance)-reionization; (c) variable-time NR at 0.45 μs neutral lifetime; and (d) variable-time NR at 1.32 μs neutral lifetime.

than **1H**⁺ and its isotopomers were not present as major components in the ion beam used for collisional neutralization. A likely explanation is that the less stable ion isomers formed by exothermic protonation with CH₅⁺ or H₃O⁺ were depleted by ion-molecule reactions with neutral 3-hydroxypyridine molecules present in the ion source. Ion trajectory simulations indicated that the ions underwent on average 40–50 collisions in the ion source, which should facilitate exothermic proton transfer from the less stable isomer to form **1H**⁺. This shake up by proton or deuteron transfer eventually yielded the most stable ions **1H**⁺ or their isotopomers, which were selected for collisional neutralization.

Radical Energetics. To further characterize the transient species of interest we addressed by ab initio and DFT calculations the relative energies of radicals **1H**–**7H** in their ground electronic states, excited-state manifolds, Franck-Condon energies in vertical electron capture, dissociation thresholds, and isomerization and dissociation energy barriers.

Radicals **1H**–**6H** were obtained as local energy minima by UHF/6-31G(d,p) geometry optimizations (Figure 5 and Supporting Information). An attempted geometry optimization of **7H** resulted in a barrierless exothermic dissociation to **1** and a hydrogen atom. The existence of radical **7H** is therefore not supported at this level of theory. MP2 and B3LYP single-point calculations agreed that **1H** was the most stable isomer of the (**1** + H)^{*} adducts (Table 3). The energy differences between **1H** and the less stable radicals **2H**, **5H**, **4H**, **6H**, and **3H** were within 53 kJ mol⁻¹ (Table 3).

Franck-Condon energies for vertical neutralization and ionization were calculated for **1H**⁺, **1H**, and **2H**⁺. Vertical electron capture in the *v*' = 0 state of **1H**⁺ formed **1H** with 27 kJ mol⁻¹ of vibrational energy. Vertical ionization of the *v* =

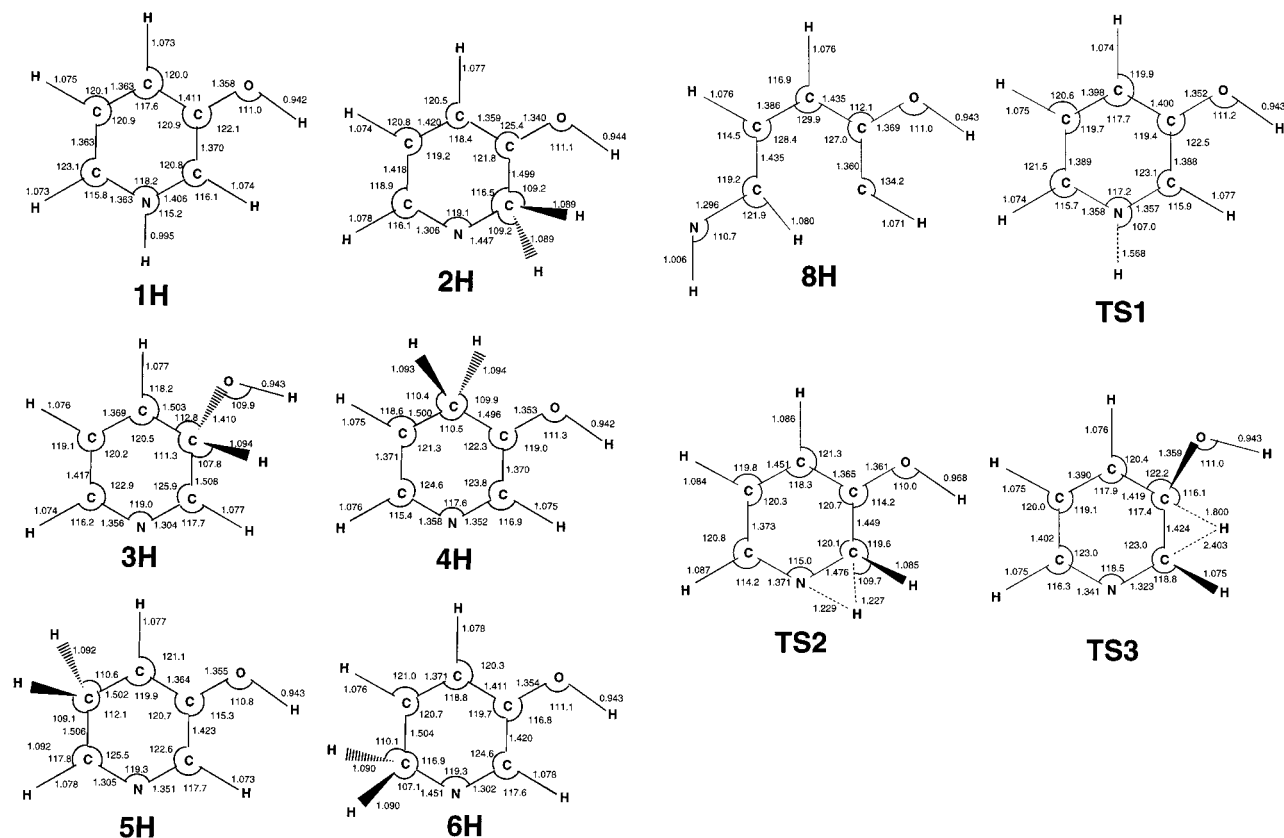


Figure 5. HF/6-31G(d,p) optimized structures of **1H**–**6H**, **8H**, **TS1**, **TS2**, and **TS3**. Bond lengths in angstroms; bond angles in degrees.

0 state of **1H** formed ion **1H⁺** with 45 kJ mol⁻¹ of vibrational energy. Vertical electron capture in vibrationally relaxed **2H⁺** formed radical **2H** with 36 kJ mol⁻¹ of vibrational energy. Hence, the Franck–Condon effects due to vertical ionization of **1H** and neutralization of **1H⁺** and **2H⁺** were only moderate.

The dissociation of the N–H bond in **1H** was investigated by stepwise energy calculations along the reaction coordinate. A transition state (**TS1**) was located at $d(\text{N–H}) = 1.568 \text{ \AA}$ (Figure 5). Single-point calculations and zero-point energy corrections gave the 0 K energy of **TS1** as 126 kJ mol⁻¹ above **1H**. The bond dissociation energy, **1H** → **1** + H[•], was 99 and 102 kJ mol⁻¹ at 0 and 298 K, respectively. Hence, the energy barrier for the reverse addition of hydrogen atom to the nitrogen atom in **1** was 27 kJ mol⁻¹.

The addition of H[•] to the nitrogen atom in **1** can be described by mixing the semioccupied 1s atomic orbital on the hydrogen atom with the lowest unoccupied molecular orbital (LUMO) of **1** (Figure 6). The orbital interactions in the hydrogen atom addition to **1** and the energy barrier were very similar to those for H atom addition to pyridine ($E_{\text{TS1}} = 27 \text{ kJ mol}^{-1}$).⁷ The potential energy barrier for the addition was probably due to electron reorganization caused by mixing a small component of HOMO with LUMO in **1** in the course of developing the SOMO in **TS1** (Figure 6).

Other unimolecular reactions of **1H** required substantial potential energy barriers. Hydrogen atom migration from N-1 to C-2 to form **2H** required 174 kJ mol⁻¹ above **1H** in the transition state (**TS2**, Figure 7). Cleavage of the N-1–C-2 bond in **1H** formed an open-ring radical **8H**, which was 223 kJ mol⁻¹ less stable than **1H** at 0 K. Since **8H** was a local energy minimum, it must be separated from the more stable **1H** by an additional potential energy barrier. Hence, a ring cleavage in **1H** en route to the formation of C₂H₂, C₃H₃, and C₂H₄N was a high-energy process. A high threshold energy was also calcu-

lated for the extrusion of **•C–OH** to form pyrrole, which required 256 kJ mol⁻¹ above **1H** at 0 K.

Loss of hydroxyl from **1H** to give pyridine was the only dissociation that had a thermochemical threshold (103 kJ mol⁻¹ at 0 K, Figure 7) comparable to that for loss of H. However, the formation of pyridine required prior hydrogen migrations, e.g., **1H** → **2H** → **3H**, which both had substantial potential energy barriers. That for the **2H** → **3H** isomerization (**TS3**) was calculated at 140 kJ mol⁻¹ above **1H** (Figure 7). A direct loss of OH[•] from **1H** would produce azacyclohexatriene-3-ylidene (pyridine 3-ylide), which was expected to be about 200 kJ mol⁻¹ less stable than pyridine by analogy with pyridine 2-ylide.³⁸ Hence, cleavage of the N–H bond was by far the lowest-energy dissociation of **1H**.

The potential energy diagram in Figure 7 also allowed an assessment of radical additions to pyridine and **1**. Addition of OH[•] to C-3 in pyridine was a barrierless process at the present level of theory. Although a transition state for the addition was located by UHF/6-31G(d,p) calculations, single-point energies at the Hartree–Fock saddle point were slightly lower than the combined energies of the pyridine and hydroxyl radical. This result was consistent with the previous observation of OH addition to C-3 in pyridine on pulse radiolysis.^{22g} A further isomerization of **3H** to **2H** required a barrier of 92 kJ mol⁻¹ (Figure 7). This barrier is substantially higher than the thresholds for both the reverse dissociation of **3H** to pyridine and OH, and the loss of hydrogen atom to form **1** (51 kJ mol⁻¹). The high energy barrier should make the **3H** → **2H** isomerization inefficient except at high thermal energies. It should be noted that loss of H-3 from **3H** probably had an activation barrier by analogy with the similar dissociation of the 4-amino-(4H)-pyrimidinium radical.⁹ The loss of H[•] from **3H** can thus be slow

(38) Lavorato, D.; Terlouw, J. K.; Dargel, T. K.; Koch, W.; McGibbon, G. A.; Schwarz, H. *J. Am. Chem. Soc.* **1996**, *118*, 11898.

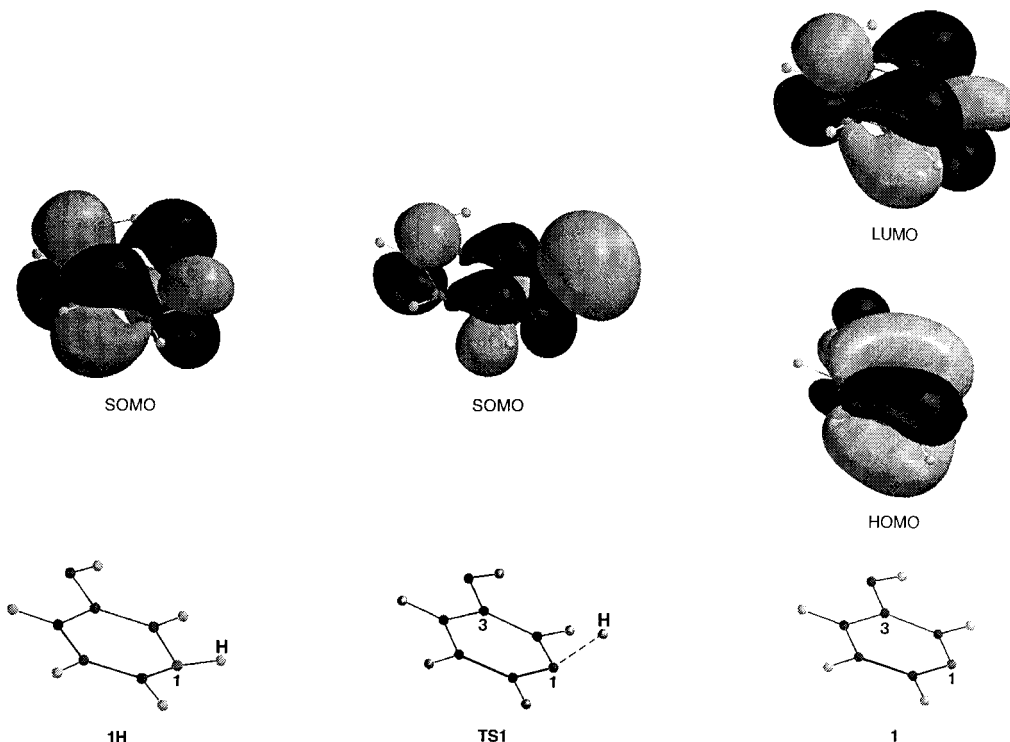


Figure 6. Frontier orbitals in **1**, **1H**, and **TS1** from HF/6-311G(2d,p) wave functions.

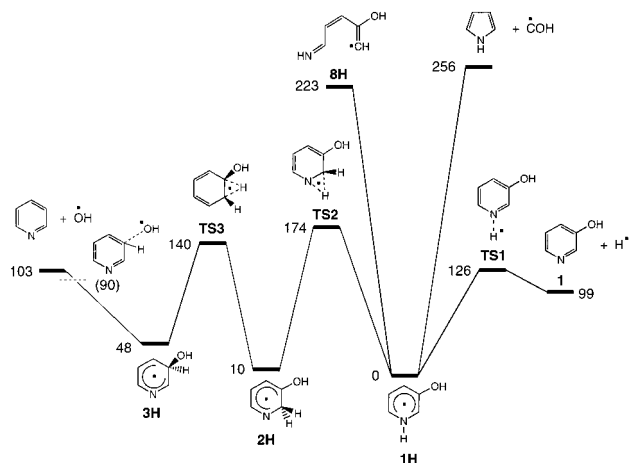


Figure 7. Potential energy diagram for dissociations and isomerizations of **1H**. Energies (kJ mol^{-1} , 0 K) are from averaged PMP2 and B3LYP/6-311G(2d,p) calculations and HF/6-31G(d,p) zero-point corrections.

enough to compete with collisional cooling provided the reaction occurred in a condensed state. Consequently, **3H** may be a detectable intermediate of OH addition to pyridine.²²

Dissociation Kinetics. The kinetics of **1H** dissociations and isomerizations were investigated with RRKM calculations by using the MP2 and B3LYP averaged energy barriers. Although the absolute values of unimolecular rate constants (k_{uni}) are known to depend strongly on the critical energies used,³⁹ the relative values are in general less susceptible to offsets in potential energies. Of particular interest were (1) the relative rates of hydrogen atom loss in **1H** versus isomerization to **2H**, (2) the magnitude of the primary isotope effect on the dissociations of the N—H and N—D bonds in **1H** and **1D**, and (3) the higher-order isotope effect on the dissociation of the N—H bonds in **1H** and **1ODH**. The calculated $k_{\text{uni}}(E)$ are shown in Figure

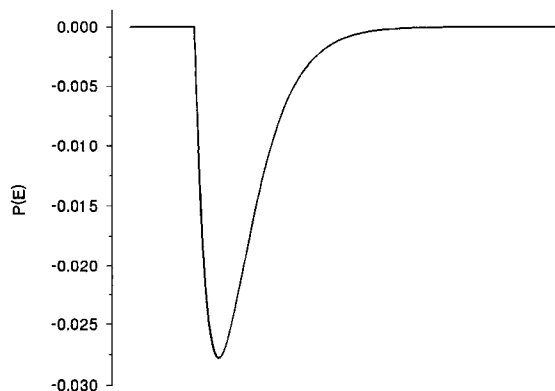
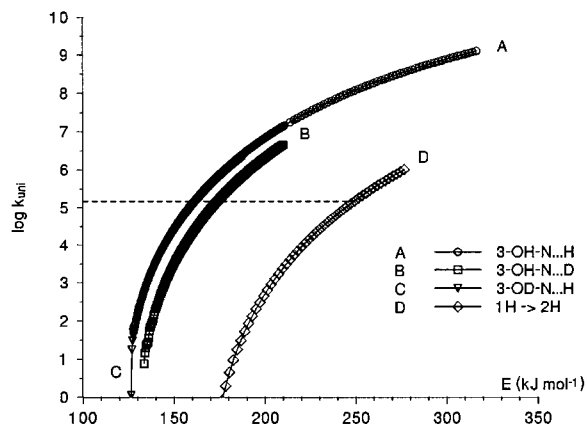


Figure 8. Top: RRKM calculated unimolecular rate constants for N—(H,D) bond dissociations of **1H**, **1ODH**, **1D**, and **1H** \rightarrow **2H** isomerization. The broken line shows $\log k$ for 50% dissociation. Bottom: Best fit internal energy distribution function for **1H**.

8. The $k(E)$ curves for the N—H and N—D bond dissociations showed relatively shallow slopes near the dissociation thresholds. For the experimental radical lifetime of 4.67 μs , 50% dissociation was achieved at $\log k_{\text{uni}} = 5.17$, as shown in Figure

(39) Gilbert, R. G.; Smith, S. C. *Theory of Unimolecular and Recombination Reactions*; Blackwell: Oxford, 1990; p 172.

8. This required kinetic shifts⁴⁰ of 35, 36, and 41 kJ mol⁻¹ for **1H**, **1ODH**, and **1D**, respectively, which increased the kinetic stability of the radicals on the time scale of the NRMS measurements.

The $k(E)$ curves further showed that the **1H** → **2H** isomerization was at least 2–3 orders of magnitude slower than the loss of H or D at all pertinent internal energies of **1H** or **1D**. This implied that dissociating **1D** could not undergo a competitive rearrangement to **2D**. Since the latter isomer but not **1D** can eliminate a light hydrogen atom (Scheme 1), the loss of D from **1D** is expected to be close to 100% specific. The loss of light hydrogen observed in the NR spectra thus must be due entirely to nonspecific ion dissociations. Available thermochemical data⁴¹ place the threshold energy for the loss of H from **1H**⁺ at 505 kJ mol⁻¹ above that for **1H**⁺. This is substantially higher than the energy barriers for proton migrations in aromatic ions (<150 kJ mol⁻¹).⁴² Hence, **1H**⁺ having sufficient internal energy to dissociate can undergo extensive scrambling of hydrogen atoms prior to loss of H, as observed in the CID spectra (vide supra).

The $k(E)$ curves indicated substantial primary isotope effects on the loss of D from **1D**, whereas the effect of OD on the loss of H from **1ODH** was negligible (Figure 8). The kinetic effects can be described by eqs 1 and 2,²⁰ where the energy distributions in **1H** and **1D** ($P_H(E)$ and $P_D(E)$) were approximated by a single $P(E)$ function (eq 3).

$$[\mathbf{1H}] = \{[\mathbf{1H}] + [\mathbf{1H} - \text{H}]\} \int P_H(E) e^{-k_H(E)\tau} dE \quad (1)$$

$$[\mathbf{1D}] = \{[\mathbf{1D}] + [\mathbf{1D} - \text{D}]\} \int P_D(E) e^{-k_D(E)\tau} dE \quad (2)$$

$$P(E) = \frac{4(E - E_0)}{W^2} e^{-2(E-E_0)/W} \quad (3)$$

Equations 1 and 2 made it possible to fit the experimental $[\mathbf{1H}]/[\mathbf{1H} - \text{H}]$ and $[\mathbf{1D}]/[\mathbf{1D} - \text{D}]$ abundance ratios with the calculated $k_H(E)$ and $k_D(E)$ by using the dissociation times $\tau = 4.67$ and $4.70 \mu\text{s}$ for **1H** and **1D**, respectively, and a $P(E)$ function (eq 3), where $E_0 = 145 \text{ kJ mol}^{-1}$ was an energy shift and $W = 26.5 \text{ kJ mol}^{-1}$ was a width parameter. Applying the $P(E)$ function from eq 3 afforded the following results: $[\mathbf{1H}]/[\mathbf{1H} - \text{H}] = 0.48$ (calculated), 0.49 (measured); $[\mathbf{1D}]/[\mathbf{1D} - \text{D}] = 1.45$ (calculated), 1.49 (measured). The best-fit distribution function showed a maximum at 158 kJ mol^{-1} and a full width at half-maximum of 33 kJ mol^{-1} (Figure 8). These properties were reasonable as shown by the following analysis. The internal energy of **1H** was composed of the internal energy of the precursor ion (**1H**⁺) and the Franck–Condon energy in vertical electron transfer. Protonation of **1** with $(\text{CH}_3)_2\text{C}-\text{OH}^+$ was 110 kJ mol^{-1} exothermic, but only ~85% of the excess reaction energy went into the ion, as predicted by the reaction dynamics simulations of Uggerud.⁴³ The internal energy in **1H**⁺ was therefore composed of the vibrational energy of **1** (38 kJ mol^{-1} at 473 K) and the fraction of protonation exothermicity, $0.85 \times 110 \approx 94 \text{ kJ mol}^{-1}$. This is an upper bound for the ion internal

energy, because the ion underwent several cooling collisions with acetone molecules in the ion source. The Franck–Condon energy in vertical neutralization of **1H**⁺ was calculated as 27 kJ mol^{-1} . The upper bound for the mean internal energy in **1H** was therefore $38 + 94 + 27 = 159 \text{ kJ mol}^{-1}$, which compared favorably with the maximum of the fitted $P(E)$ function (158 kJ mol^{-1} , vide supra).

Other types of energy distribution functions were also tried but performed worse than the one in eq 3. Symmetrical (Gaussian) and inverted Boltzmann-like $P(E)$ functions could roughly fit the experimental data only when assuming distribution maxima at energies between 210 and 230 kJ mol^{-1} . Such energy distributions were difficult to justify on the basis of the ion and electron-transfer energetics.

Considering the very facile loss of H from **1H**, the occurrence upon NR of competitive ring cleavages should be discussed. Ring fragmentations can occur competitively in **1H** with $\gg 230 \text{ kJ mol}^{-1}$ of internal energy (vide supra), in **1** formed by loss of H, and/or in **1**⁺ and **1H**⁺ following collisional reionization. However, both **1** and **1**⁺ were substantially stable, as evidenced by the NR spectrum of the latter, which showed a very abundant survivor ion, $[\mathbf{1}^{+\bullet}] = (25\%) \sum I_{\text{NR}}$ (Figure 2a). To promote ring cleavage in **1**⁺ formed by the **1H** → **1** → **1**⁺ reaction sequence would require that the energy driving these dissociations be carried over from highly energetic **1** formed by dissociation of excited **1H**. However, this was incompatible with the analysis of isotope effects on loss of H, which indicated internal energies in dissociating **1H** that would form **1** with $\sim 30 \text{ kJ mol}^{-1}$ of average internal energy. It therefore appeared that the occurrence of ring cleavages upon NR cannot be logically explained by consecutive dissociations, e.g., **1H** → **1** → **1**⁺ → ring fragments, but must be due to competitive dissociations in **1H**. Since the potential energy surface of the ground electronic state of **1H** favored loss of H, the more endothermic ring cleavages must have occurred on the surface of an excited state.⁴⁴

Excited States. The energetics of the lowest excited states of **1H** were addressed by Configuration Interaction Singles (CIS/6-311G(2d,p)) calculations.⁴⁵ Out of the five excited states investigated, the lowest two states in **1H**, A and B, were due to excitation of the odd electron from the 26α SOMO. The CIS wave function for the A state is shown in Figure 9, and the B state was described by $\Phi = 0.908(27\alpha) - 0.303(28\alpha)$. Importantly, such outer excited states can be formed directly by electron transfer to ion **1H**⁺, whereby the electron is captured within the manifold of virtual orbitals in the ion. Both the A and B electronic states had low oscillator strengths for radiative transitions to the ground (X) state, as shown for the A state in Figure 9, which also depicts the calculated adiabatic and vertical ionization energies of **1H**. The calculated radiative lifetimes for the A and B states, $\tau_{ij} = 1/A_{ij}$, where A_{ij} is the Einstein coefficient, were 0.4 and $3.4 \mu\text{s}$ for the A → X and B → X transitions, respectively. Hence, the states were sufficiently long-lived to undergo dissociations or internal conversion to a highly vibrationally excited ground electronic state **1H**. The excitation–deexcitation of the A and B states showed substantial Franck–Condon effects. Those for the A state are summarized in Figure 9. For the B state the X → B excitation of relaxed **1H** required 4.80 eV, while excitation of (X)**1H** formed by vertical neutral-

(40) Lifshitz, C. *Mass Spectrom. Rev.* **1982**, *1*, 309.

(41) From the heats of formation (kJ mol^{-1}) of **1** (−44), **1**⁺ (839), **H**⁺ (218), and **H**⁺ (1530) and the proton affinity of **1** (922).

(42) For a discussion of energy barriers to proton migrations in aromatic ions see: (a) Mason, R.; Milton, D.; Harris, F. *J. Chem. Soc., Chem. Commun.* **1987**, 1453. (b) Hrusak, J.; Schroder, D.; Weiske, T.; Schwarz, H. *J. Am. Chem. Soc.* **1993**, *115*, 2015. (c) Glukhovtsev, M. N.; Pross, A.; Nicolaides, A.; Radom, L. *J. Chem. Soc., Chem. Commun.* **1995**, 2347. (d) Szulejko, J. E.; Hrusak, J.; McMahon, T. B. *J. Mass Spectrom.* **1997**, *32*, 494.

(43) Uggerud, E. *Adv. Mass Spectrom.* **1995**, *13*, 53.

(44) For a discussion of the role of excited electronic states in collisional electron transfer see: (a) Frank, A. J.; Sadilek, M.; Ferrier, J. G.; Turecek, F. *J. Am. Chem. Soc.* **1997**, *119*, 12343. (b) Sadilek, M.; Turecek, F. *J. Phys. Chem.* **1996**, *100*, 15027. (c) Sadilek, M.; Turecek, F. *Chem. Phys. Lett.* **1996**, *263*, 203. (d) Sadilek, M.; Turecek, F. *J. Phys. Chem.* **1996**, *100*, 224.

(45) Foresman, J. B.; Head-Gordon, M.; Pople, J. A.; Frisch, M. J. *J. Phys. Chem.* **1992**, *96*, 135.

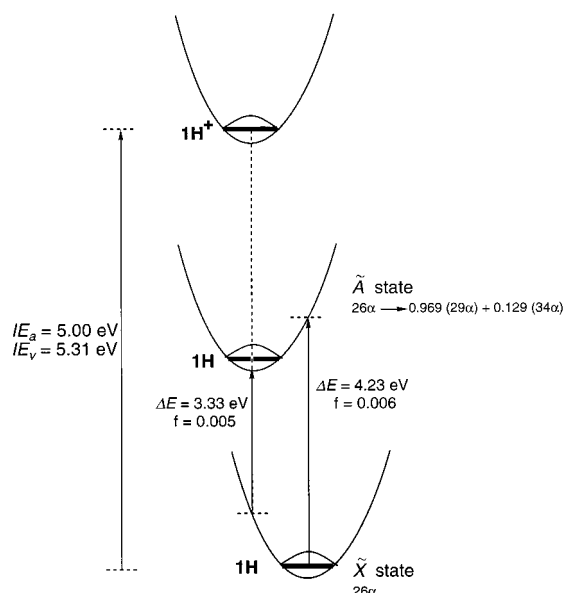


Figure 9. Potential energy diagram for ionization and X \rightarrow A electronic excitation in **1H**. Excitation energies and oscillator strengths are from CIS/6-311G(2d,p) calculations. Ionization energies are from averaged PMP2 + B3LYP/6-311G(2d,p) calculations.

ization of **1H**⁺ required 3.7 eV. This suggested that the potential energy surfaces of the A and B states were shifted with respect to that of the X state. Such shifts should favor internal conversion to form the vibrationally hot X state because of the proximity of the potential energy surfaces.⁴⁶ It is currently unknown whether ring cleavages occurred adiabatically in electronic excited states of **1H** or in a vibrationally hot ground state. It is also conceivable but not proven that the electronic

(46) Turro, N. J. *Modern Molecular Photochemistry*; University Science Books: Mill Valley, 1991; pp 70–75.

energy in the A or B state can be used to produce an open-ring photoisomer of **1H** which will then dissociate extensively upon collisional ionization. Although the details of energy storage and conversion in **1H** remain to be elucidated, the existence of long-lived outer excited electronic states of **1H** provides a mechanism for the formation of high-energy **1H** in which ring cleavages are energetically possible.

Conclusions

3-Hydroxy-(1*H*)-pyridinium radical (**1H**) was the most stable isomer of the hydrogen atom adducts to 3-hydroxypyridine. Radical **1H** was formed as a stable species by vertical neutralization of cation **1H**⁺. Loss of hydrogen atom from **1H** was the lowest-energy dissociation. In the gas phase this dissociation showed a substantial kinetic shift and primary deuterium isotope effect that increased the kinetic stability of **1H** and **1D**. Ring-cleavage dissociations of **1H** were substantially more endothermic than loss of hydrogen atom and could proceed competitively in **1H** formed in excited electronic states. Other hydrogen atom adducts to the pyridine nucleus in 3-hydroxypyridine were calculated to be stable radicals that required substantial energy barriers to isomerizations by 1,2-hydrogen atom migrations.

Acknowledgment. Support by the National Science Foundation (CHE-9712570) is gratefully acknowledged. We thank Drs. Lars Frosig (University of Copenhagen) and Martin Sadilek (University of Washington) for CID spectra measurements.

Supporting Information Available: Tables of MP2/6-311G(d,p) and B3LYP//6-311G(2d,p) total energies, HF/6-31G(d,p) optimized geometries, and uncorrected harmonic frequencies. This material is available free of charge via the Internet at <http://pubs.acs.org>.

JA983789A